TIDAL DISSIPATION DUE TO DESPINNING AND THE EQUATORIAL RIDGE ON IAPETUS. James H. Roberts, *Johns Hopkins University Applied Physics Lab, Laurel, MD 20723 (James.Roberts@jhuapl.edu)*, Francis Nimmo, *Department of Earth and Planetary Sciences, University of California at Santa Cruz, Santa Cruz, CA 95064, USA,*.

Introduction: The equatorial ridge on Iapetus is a geological anomaly in the solar system. This ridge is 20 km high and spans more than half the circumference of Iapetus [1]. Multiple hypotheses have been suggested for the origin of this ridge including convective upwelling in the underlying ice shell [2], the remains of an early ring system [3], and a giant thrust fault as the satellite contracted and despun from a faster initial rotation rate [4]. Despinning may result in large compressive stresses at the equator [5], but the principal stresses in this case are not oriented in the direction needed to produce an equatorial ridge. Here we investigate whether tidal dissipation due to early despinning of Iapetus may promote formation of a degree-2 convective upwelling in the ice shell that may form the ridge dynamically.

Despinning Stresses: Presumably, Iapetus formed as an oblate spheroid in hydrostatic equilibrium with some flattening f. The departure from a sphere is caused by the centipetal acceleration due to rotation, and a gravitational perturbation arising from the deformed mass [5]. The hydrostatic flattening for a rotating body is

$$f = \frac{\frac{5}{2}m}{1 + \left[\frac{5}{2}\left(1 - \frac{3}{2}(C/(MR^2))\right)\right]^2} \quad (1)$$

where $m = (\omega^2 R^3)/(GM)$, C is the polar moment of inertia, M is the mass of Iapetus, R is the mean radius, G is the gravitational constant, and ω is the rotation rate [6]. During despinning, m decreases. However, as Iapetus cools, a lithosphere capable of supporting elastic stresses forms and resists changes in shape due to despinning. Thus, the new value of f does not necessarily satisfy eq. 1, and stresses accumulate in the lithosphere. Melosh [5] showed that despinning of an elastic spheroid results in a characterstic stress pattern that promotes the formation of three distinct provinces of fractures at the surface: extension at the poles, strike-slip faults at mid-latitudes, and equatorial thrust faults (see fig. 1 from [5]). However, the azimuthal stresses are always larger than meridional stresses, and the equatorial faults strike north-south. Thus, despinning stresses alone cannot form the east-west equatorial ridge.

Tidal Dissipation from Despinning: The shape of Iapetus is consistent with a hydrostatic body with a 16 h rotation period [4]. The tide on Iapetus raised by Saturn leads the planet, and generates a tidal torque which acts to slow the rotation of Iapetus and transfers the angular momentum into the orbital revolution. Energy is not conserved in this exchange and the excess energy ΔE is dissipated as heat in the satellite's interior [7]. The orbital evolution continues until the satellite rotates synchronously. The timescale for the despinning τ_d is a function of the mechanical and orbital properties [4,7]:

$$\tau_d = -\frac{\omega C a^6}{3\mathrm{Im}(k_2) G M_S^2 R^5} \quad (2)$$

where a is the semimajor axis, M_S is the mass of Saturn, and k_2 is the complex degree-2 Love number. τ_d for Iapetus is expected to be on the order of 10^8 y. From this, we can determine the mean global dissipation rate $\dot{E} = \Delta E/\tau_d$. However, heating of the interior is not uniform, and is controlled by the deformation and stress pattern.

As discussed above, Melosh [5] provides a formulation for stresses and deformation in response to despinning for both a homogeneous elastic sphere, and for an elastic shell above a fluid interior. We modify this approach to consider a Maxwellian viscoelastic body, characterized by a complex rigidity $\tilde{\mu} = (\eta\omega\mu^2 + i\eta^2\omega^2\mu)/(\eta^2\omega^2 + \mu^2)$, where η is the viscosity, and μ is the shear modulus [8]. We then compute the complex strains ϵ_{ij} and stresses σ_{ij} as in [5], and the resultant tidal dissipation rate $H = \sigma_{ij}\dot{\epsilon}_{ij}$ for the period of despinning [9]. For constant despinning, $\dot{\epsilon}_{ij} = (\epsilon_{ij}/\tau_d)$. An example of the heating pattern is shown in Fig. 1 for a differentiated Iapetus. Heating is strongest in the deep interior at 45° latitude, but in the near-surface is strongest near the equator, potentially promoting equatorial upwellings [10].

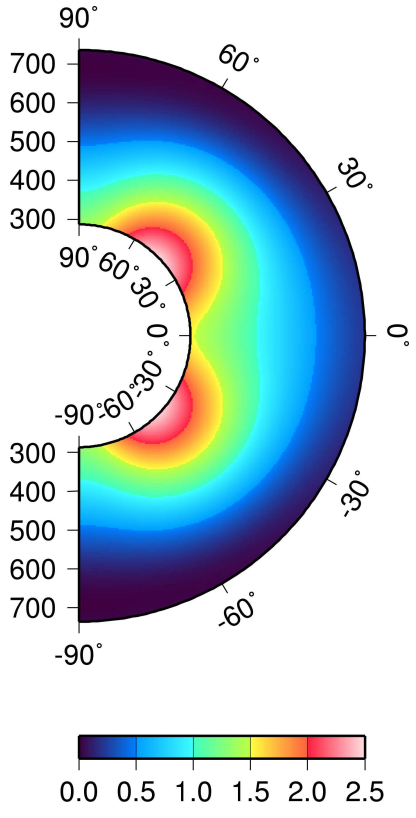

Figure 1: Volumetric heat production rate (in 10^{-9} W m^{-3}) in the ice shell of a fully differentiated Iapetus. $\eta = 10^{14}$ Pa s, μ = 4 GPa.

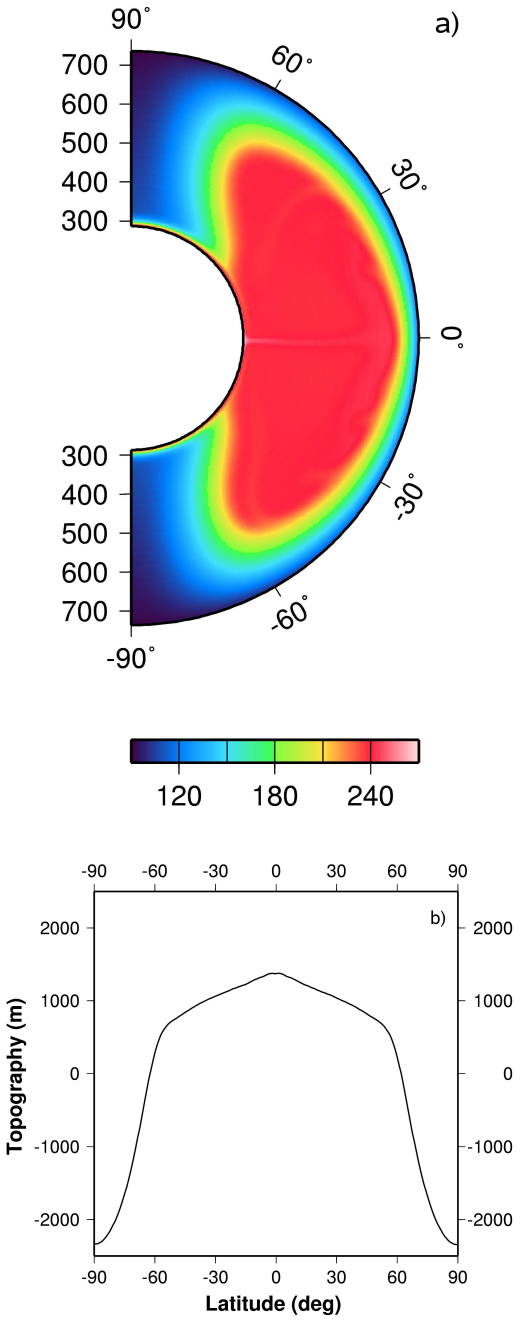

Figure 2: Temperature in K (a) and dynamic topography (b) for the case shown in Fig. 1 at 500 Ma model time, well after the despinning.

We model dynamics of the ice shell using Citcom [11], a 2D axisymmetric finite-element code, using temperature-dependent viscosity. We apply free-slip boundary conditions at the boundaries of the ice shell. The bottom is isothermal and the surface temperature varies with latitude. The spatial pattern of heating due to despinning stresses is computed as described above and this heating is included until the model time exceeds the despinning timescale.

Results: Preliminary findings indicate that the despinning heat and strong viscosity gradients results in a primarily degree-2 convection pattern with a large-scale upwelling at the equator and downwellings at the poles (see Fig. 2a). Because the model is axisymmetric, this upwelling is really a ring shape. This upwelling creates substantial dynamic topography at the surface reflecting the underlying convective pattern. The dynamic topography at equatorial latitudes is a few km higher than the poles (see Fig. 2b).

Discussion: While our models produce elevated topography at the equator, we note there remain significant differences between our models and the observed ridge on Iapetus. In particular, the actual ridge is much taller and narrower that the one shown in Fig. 2b. However, our results at this stage are preliminary and additional physics will be included as part of the ongoing investigation. One important mechanism may be plastic yielding, which is expected to concentrate the deformation and increase the topography locally. Alternatively, the upwelling may lead to preferential melting at the equator, which can result in dikes. Such extentional features are expected to trend east-west at the equator [12].

Further simplifications will be relaxed as the work continues. Currently, the despinning is assumed to proceed linearly, and thus the local heating rate is constant until the despinning is complete. In reality, the despinning is time-dependent and the instantaneous rotation, flattening, strain, and heating rate should be recalculated at each timestep. The elastic strain models of Melosh [5] are for a homogeneous or spherically symmetric body. Because strong lateral viscosity variations may exist in a convecting ice shell, the heating will be affected by the local viscosity. This viscosity-dependence will be included by means of a perturbation factor as in [13,14].

Although despinning stresses [5] alone cannot form an equatorial ridge such as that seen on Iapetus, preliminary results suggest that the heat produced by these stresses can promote the formation a degree-2 pattern of convection with an equatorial upwelling. Developing a permanent, narrow ridge from the broader, short-lived dynamically-supported equatorial topography requires additional effects, such as either plasic yielding of near-surface ice or intrusion of warm, low-density ice (diking) [12].

References: [1] Dombard, A. J. and A. F. Cheng (2008) *LPSC 39*, 2262. [2] Czechowski, L. and J. Leliwa-Kopystynski (2008) *Adv. Space Res., 42*, 61-69. [3] Ip, W. H. (2006) *GRL, 33*, 16203. [4] Castillo-Rogez, J. C. et al. (2007) *Icarus, 190*, 179-202. [5] Melosh, H. J. (1977) *Icarus, 31*, 221-243. [6] Jeffreys, H. (1952) *The Earth*, Cambridge Univ. Press. [7] Goldreich, P. and S. Soter (1966) *Icarus, 5*, 375-389. [8] Zschau, J. (1978) in *Tidal Frication and the Earth's Rotation*, Springer-Verlag. [9] Peale, S. J. and P. Cassen (1978) *Icarus, 36*, 245-269. [10] Roberts, J. H. and F. Nimmo (2008) *GRL, 35*, L09201. [11] Roberts, J. H. and S. Zhong (2004) *JGR, 109*, E03009. [12] Melosh, H. J. (2008) *LPSC, 40*, this volume. [13] Sotin, C. et al. (2002) *GRL* 29, 1233. [14] Roberts, J. H. and F. Nimmo (2008) *Icarus* 194, 675-689.